

Dual Fluorescent Labelling of Cellulose Nanocrystals for pH sensing

Lise Junker Nielsen,^a Samuel Eyley,^b Wim Thielemans^b and Jonathan W. Aylott^{*c}

^a *CelCom, Department of Biochemistry and Molecular Biology, University of Southern Denmark, Campusvej 55, DK-5230 Odense M, Denmark*

^b *Inorganic & Materials Chemistry, School of Chemistry and Process & Environmental Research Division – Faculty of Engineering, University of Nottingham, University Park, Nottingham, UK NG7 2RD*

^c *School of Pharmacy, Boots Science Building, University of Nottingham, University Park, Nottingham, UK NG7 2RD*
E-mail: jon.aylott@nottingham.ac.uk

Materials

Flourescein-5'-isothiocyanate (FITC) (90%), and dichloromethane (extra dry, Acroseal) were obtained from Acros Organics, Rhodamine B isothiocyanate (RBITC) was obtained for MP Biomedicals, Oregon Green 488 carboxylic acid, succinimidyl ester (OG-SE) and 5-(and-6)-carboxytetramethylrhodamine succinimidyl ester (TAMRA-SE) were obtained from Invitrogen, N,N'-diisopropylcarbodiimide was obtained from Alfa Aesar (Johnson Matthey), dichloromethane, ethanol, sulfuric acid and cotton wool were obtained from Fisher Scientific (UK), 4-dimethylaminopyridine was obtained from Fluka, 5-(and-6)-carboxyfluorescein succinimidyl ester (FAM-SE) (90%) and all other reagents were obtained from Sigma Aldrich, and all reagents were used without further purification. Deionized water was purified by an Elga PURELAB Maxima HPLC to 18.2 M Ω -cm.

Analysis

FT-IR analyses were conducted on a Thermo-Nicolet 380, and analysed with OMNIC software. XPS analyses were performed with a Kratos AXIS ULTRA spectrometer using a monochromated Al K α X-ray source ($h\nu = 1486.6$ eV), and a delay line detector (DLD) with a takeoff angle of 90° and an acceptance angle of 30°. The X-ray gun power was set to 120 W. The spectra were recorded in fixed analyser transmission mode using an aperture slot of 300 \times 700 μm^2 with a pass energy of 80 eV for survey scans and 20 eV for high-resolution scans. Charge neutralization was performed using a low energy electron gun within the field of the magnetic lens. All spectra were recorded using Kratos VISION II software and processed using CasaXPS software, binding energies were referenced to aliphatic carbon 1s at 284.8 eV. Elemental analyses were performed in the microanalysis service of the School of Chemistry, with a CE-440 elemental analyzer manufactured by Exeter Analytical. X-ray Diffraction studies were performed using a PANalytical X'Pert Pro MPD in Bragg-Brentano geometry, with monochromated Cu K α_1 ($\lambda = 1.5406$ Å, 40 kV, 40 mA) radiation, automated divergence and receiving slits (10 mm illuminated length), 10 mm beam mask, 0.04 rad soller slits and a step size of 0.08°. Fluorescence was measured at $\lambda_{\text{ex}} = 540/5$ nm, $\lambda_{\text{em}} = 573/5$ nm for RBITC using a Varian Cary Eclipse fluorescence spectrophotometer. UV/Vis spectra were recorded using a Varian Cary 50

UV-Vis spectrophotometer. Sample concentration was 0.1 wt % for both fluorescence and UV-Vis measurements.

AFM images were obtained in tapping mode at room temperature using a Veeco Nanoscope IIIa Multimode AFM with a Veeco RSTEP cantilever with a spring constant of 40 N/m and resonance frequency of 279 kHz. Samples were prepared by depositing 20 μ L of a 0.001 wt % solution of nanocrystals filtered through a 0.45 μ m syringe filter onto freshly cleaved mica followed by air-drying.

Experimental procedures

Preparation of cellulose nanocrystals: Pure cotton (cotton wool) was dispersed in 64 wt% sulfuric acid in water. This suspension was held at 45 °C under mechanical stirring for 35 min to allow cotton hydrolysis. The suspension was subsequently diluted with an equal part of cold water and washed by successive centrifugation at 10,000 rpm and 10 °C (three times). Dialysis against tap water was performed to remove free acid in the dispersion. This was verified by neutrality of the dialysis effluent. The nanocrystals were then recovered by freeze-drying after dispersion in water using a Branson Sonifier and filtration over a No. 2 fritted glass filter to remove residual aggregates and treatment with Amberlite MB 6113 mixed bed ion exchange resin to remove residual ions from the water.

Preparation of FITC/RBITC labelled cellulose nanocrystals: Cellulose nanocrystals (250 mg) were suspended in 25 mL of 0.1 M NaOH along with 7.5 mg of RBITC and 10 mg of FITC and stirred for 4.5 days in the dark at RT. The suspension was centrifuged (15 min, 6000 rpm) and the orange supernatant discarded. The precipitate was washed with 0.1 M NaOH (4 \times 40 mL), dialyzed against deionized water for 2 days and freeze dried.

X-ray diffraction

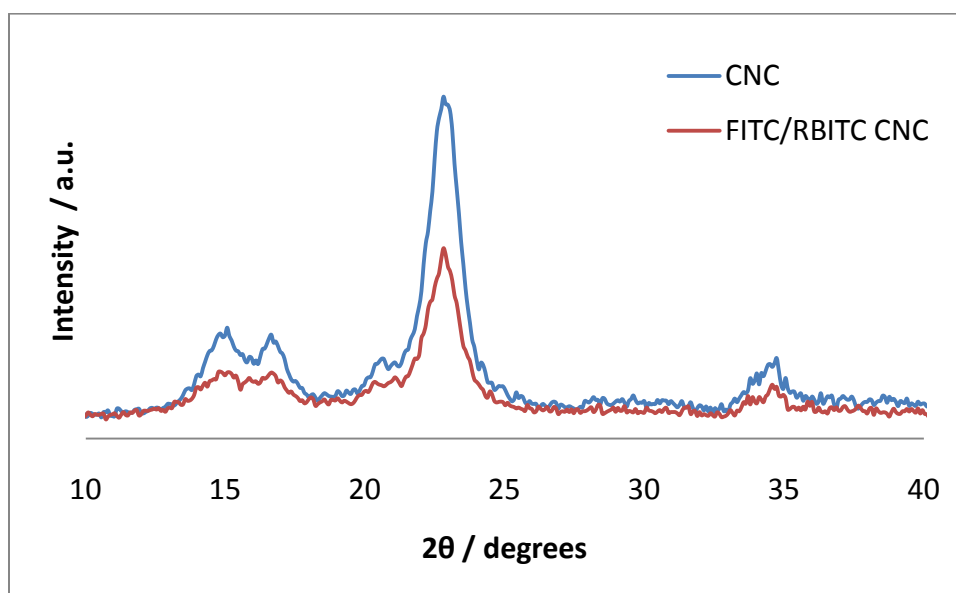


Figure S1: X-ray diffraction data for unmodified cellulose nanocrystals (CNC) and cellulose nanocrystals labeled with FITC and RBITC (FITC/RBITC CNC).

Figure S1 shows the XRD diffraction patterns of the cellulose nanocrystals before and after modification. Both before and after modification the pattern shows a clear Cellulose I β polymorph with the 200 diffraction centered around 22.7°, and the double peak signal at 14.5° and 16° for 110 and 1 $\bar{1}$ 0 respectively. A small peak around 20° due to 102 diffraction is also noticed. The crystallinity index¹ was determined to be 88% and 85% before and after modification respectively, showing that the crystal structure is essentially not affected by the grafting of the dyes or the reaction conditions as the differences in crystallinity index is within experimental error.

AFM

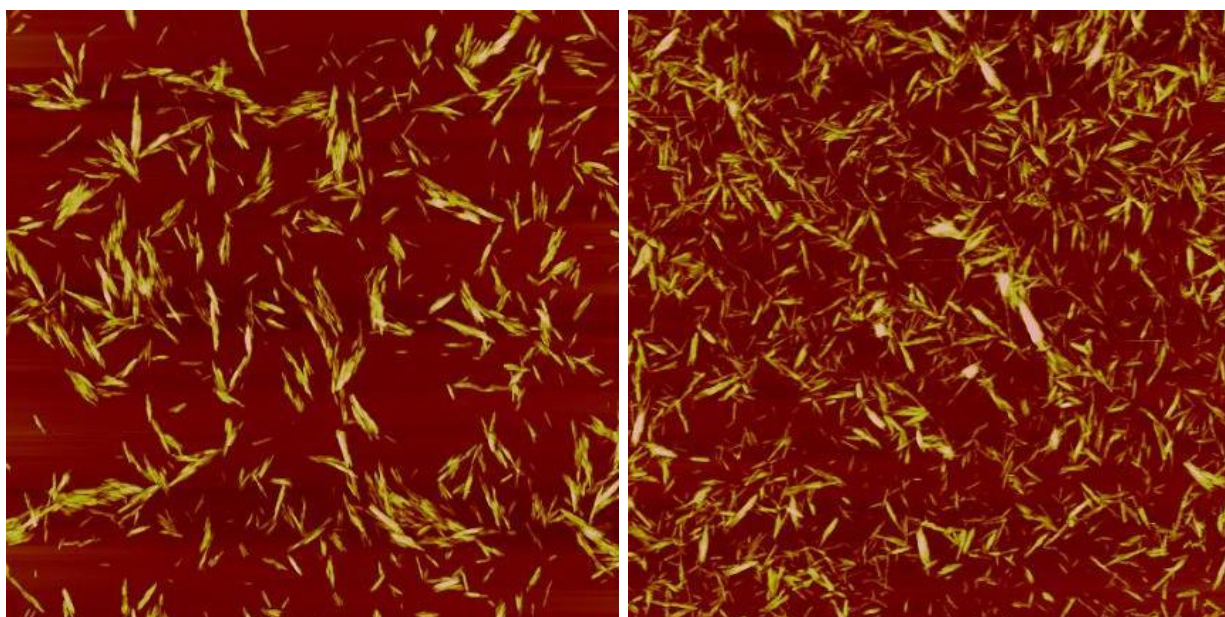


Figure S2: AFM images of cellulose nanocrystals (left) and FITC/RBITC cellulose nanocrystals (right) with a 5 μ m scan size.

Figure S2 shows the AFM images of the cellulose nanocrystals before and after modification. As can be seen in the images the needle-like morphology of the cellulose nanocrystals has been retained.

Determination of grafting density

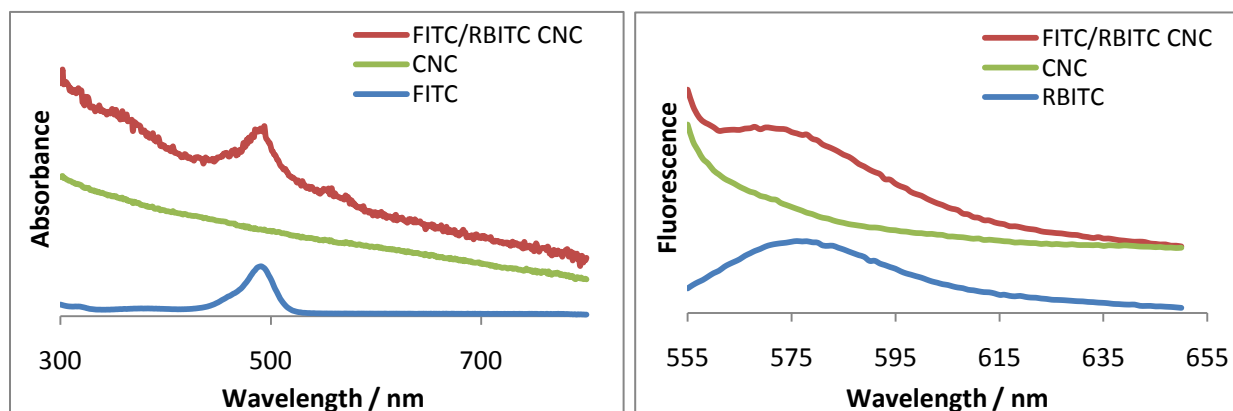


Figure S3: UV-Vis (left) and fluorescence (right) spectra of unmodified (0.1 wt %) and modified cellulose nanocrystals (0.1 wt %) and naked dye (2.5 μ M) in 0.1 M NaOH.

The grafting density of FITC and RBITC was determined by UV-Vis and fluorescence spectroscopy, respectively. As can be seen in Figure S3 the modified nanocrystals show a clear absorbance peak at 490 nm corresponding to FITC and a clear emission peak at 580 nm for RBITC, whereas the unmodified cellulose nanocrystals show no absorption or emission peaks at these wavelengths. The grafting density was determined by relating the intensity of the peaks to a calibration curve constructed from known concentrations of the free dye in 0.1 M NaOH.

Preparation of methacrylate cellulose nanocrystals (M CNC): Cellulose nanocrystals (570 mg) were suspended in 20 mL of dry DCM under argon along with 5 mg of DMAP. Methacrylic acid (0.42 mL) and DIC (0.8 mL) was added sequentially and the reaction was stirred for 5 days at RT. The suspension was filtered and the solid was purified by successive Soxhlet extractions with DCM (24 h) and ethanol (24 h) and dried *in vacuo*.

Preparation of amine cellulose nanocrystals (A CNC): Methacrylate cellulose nanocrystals (250 mg) were suspended in 55 mL methanol along with 48 mg of cysteamine, and stirred for 3 days at RT. The suspension was centrifuged (10 min, 6000 rpm) and the supernatant discarded. The precipitate was washed with methanol (3 × 40 mL) and dried *in vacuo*.

Preparation of FAM-SE/TAMRA-SE and OG-SE/TAMRA-SE labelled cellulose nanocrystals (F L CNC): Amine cellulose nanocrystals (100 mg) were suspended in 25 mL of 50 mM sodium borate buffer pH = 9.0 along with 2.0 mg of TAMRA-SE and 3.2 mg of FAM-SE (2.0 mg OG-SE) and stirred for 24 h in the dark at RT. The suspension was centrifuged (10 min, 6000 rpm) and the supernatant discarded. The precipitate was washed with 50 mM sodium borate buffer pH = 9.0 (3 × 40 mL), dialyzed against deionized water for 2 days and freeze dried.

X-ray diffraction

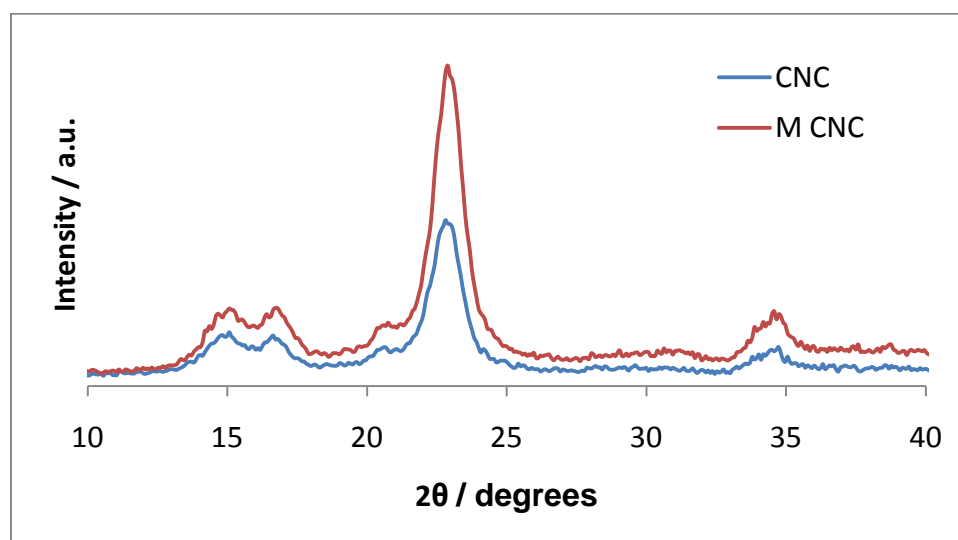


Figure S4: X-ray diffraction data for unmodified cellulose nanocrystals (CNC) and methacrylate cellulose nanocrystals (M CNC).

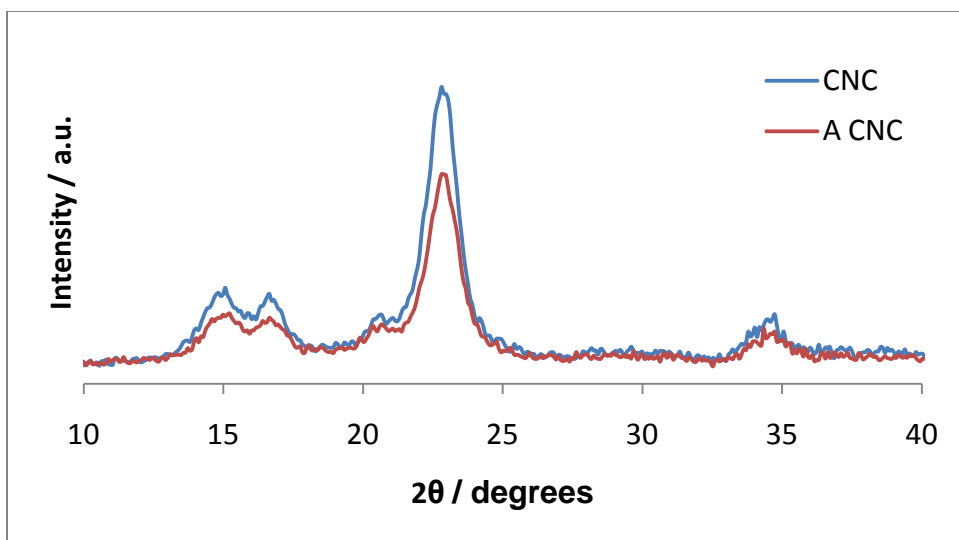


Figure S5: X-ray diffraction data for unmodified cellulose nanocrystals (CNC) and amine cellulose nanocrystals (A CNC).

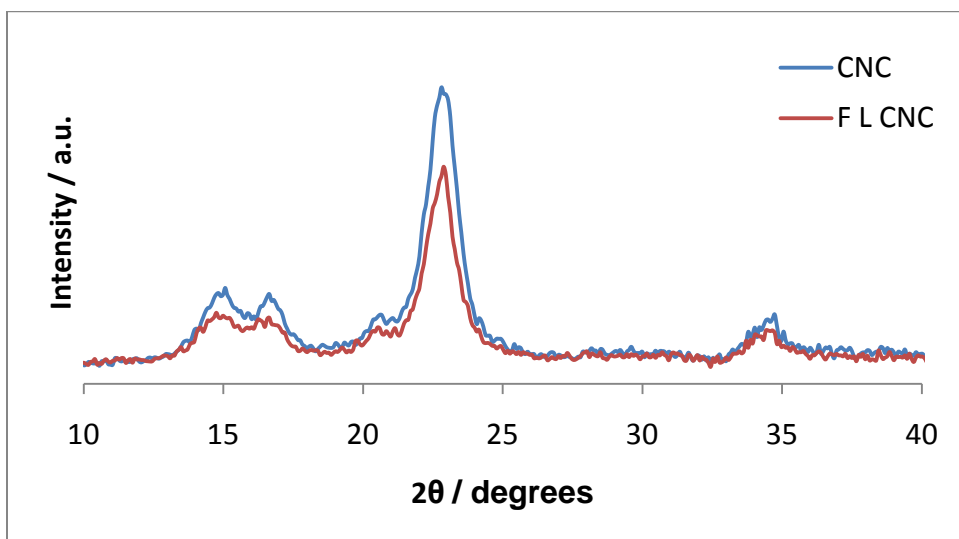


Figure S6: X-ray diffraction data for unmodified cellulose nanocrystals (CNC) and fluorescently labelled cellulose nanocrystals (F L CNC).

Figure S5, S6 and S7 show the XRD diffraction patterns of the cellulose nanocrystals before and after each modification. As seen previously both before and after modification the pattern shows a clear Cellulose I_{β} polymorph with the 200 diffraction centered around 22.7° , and the double peak signal at 14.5° and 16° for 110 and $1\bar{1}0$ respectively. A small peak around 20° due to 102 diffraction is also noticed. The crystallinity index was determined to be 89%, 85% and 86% for the three modifications (M CNC, A CNC and F L CNC), showing that the crystal structure is essentially not affected by the grafting of the dyes or the reaction conditions, as the differences in crystallinity index as compared to the unmodified cellulose nanocrystals (88%) is within experimental error.

AFM

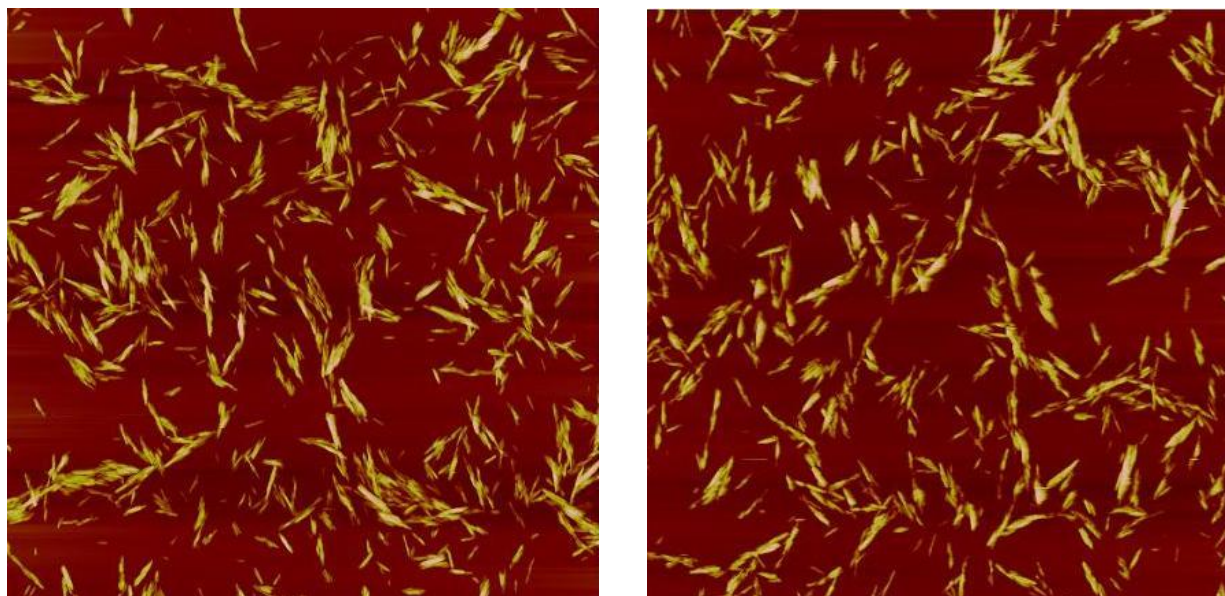


Figure S7: AFM images of cellulose nanocrystals (left) and fluorescently labelled cellulose nanocrystals (right) with a 5 μm scan size.

Figure S8 shows the AFM images of the cellulose nanocrystals before and after modification. As can be seen in the images the needle-like morphology of the cellulose nanocrystals has been retained.

FT-IR

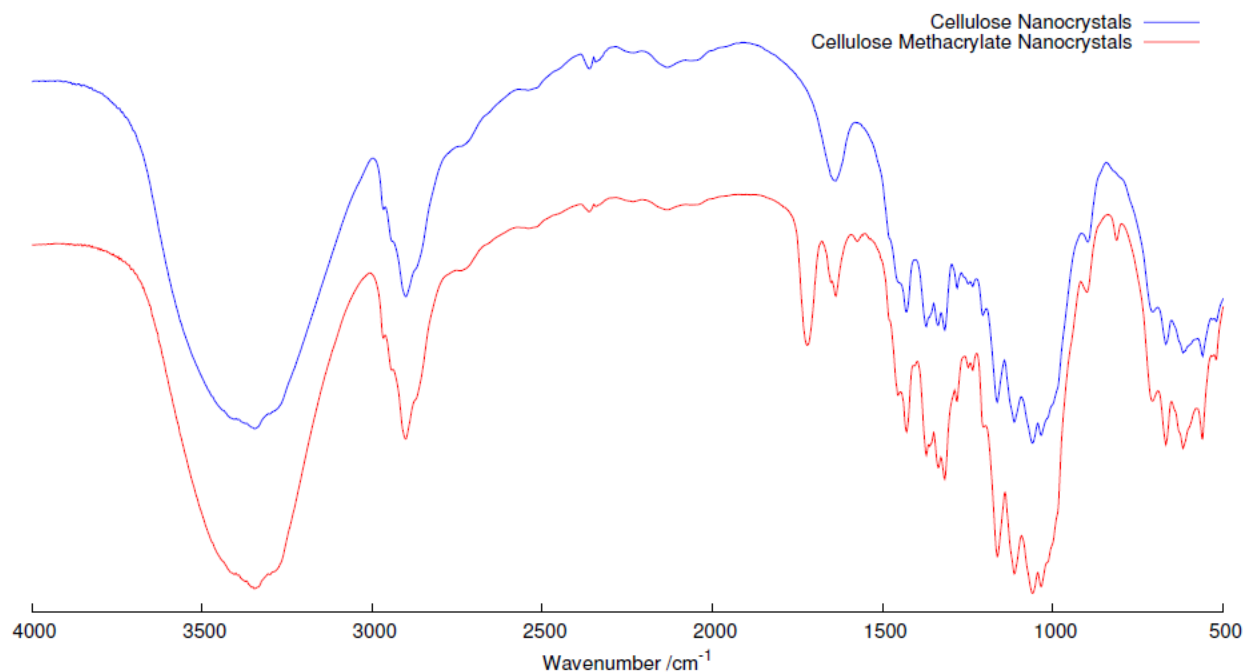


Figure S8: FT-IR spectra of the methacrylate cellulose nanocrystals and the unmodified cellulose nanocrystals.

The FT-IR spectra in Figure S8 clearly show the successful grafting of the methacrylic acid to the cellulose nanocrystals by the appearance of a peak at 1715 cm^{-1} corresponding to the $\nu(\text{C}=\text{O})$ of the ester.

XPS and elemental analysis

Table 1: Analysis of XPS Survey Scans

| | C 1s / At % | O 1s / At % | N 1s / At % | S 2p / At % | F 1s / At % |
|-------------------------------------|-------------|-------------|-------------|-------------|-------------|
| Cellulose Nanocrystals | 59.5 | 40.5 | - | - | - |
| Methacrylate Cellulose Nanocrystals | 62.3 | 37.7 | - | - | - |
| Amine Cellulose Nanocrystals | 62.0 | 35.9 | 1.3 | 0.8 | - |
| OG-SE/TAMRA-SE Labelled | 60.9 | 36.4 | 1.5 | 0.6 | 0.6 |

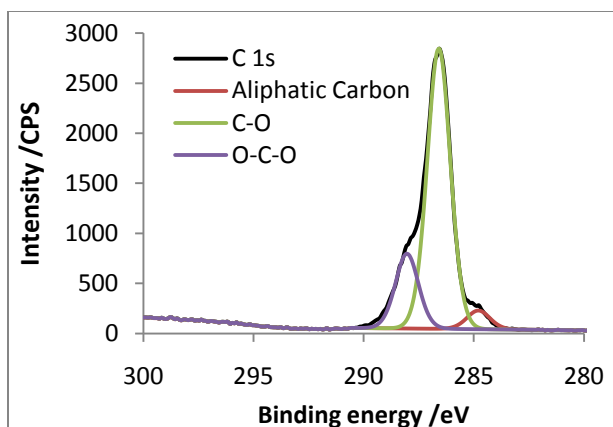


Figure S9: High resolution spectra of the C 1s peak.

Table 2: Peak Fitting Carbon 1s in Cellulose Nanocrystals

| Environment | Binding Energy /eV | FWHM | Lineshape* |
|--------------------|--------------------|------|------------|
| C-C (Adventitious) | 284.8 | 1.23 | GL(30) |
| C-O | 286.6 | 1.23 | GL(30) |
| O-C-O | 288.0 | 1.23 | GL(30) |

*GL(m) corresponds to a Gaussian Lorentzian mixed function with m indicating the % Lorentzian character.

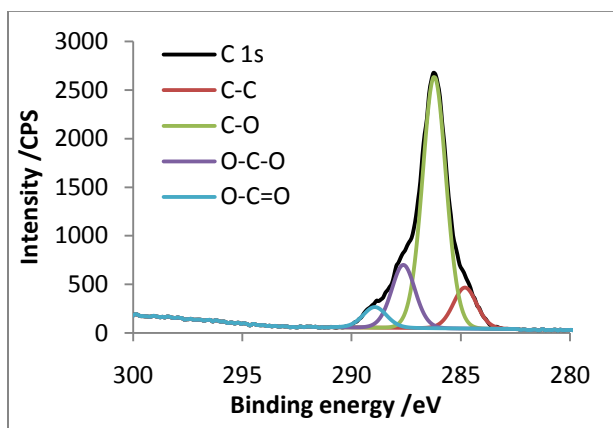


Figure S10: High resolution spectra of the C 1s peak for Methacrylate Cellulose Nanocrystals.

Table 3: Peak Fitting Carbon 1s in Methacrylate Cellulose Nanocrystals

| Environment | Binding Energy /eV | FWHM | Lineshape |
|-------------|--------------------|------|-----------|
| C-C/C=C | 284.8 | 1.26 | GL(30) |
| C-O | 286.2 | 1.26 | GL(30) |
| O-C-O | 287.6 | 1.26 | GL(30) |
| O-C=O | 288.9 | 1.26 | GL(30) |

When comparing the XPS spectra of the unmodified cellulose with the methacrylate cellulose we can clearly see the appearance of signals from the ester group in the C 1s peak, further confirming the successful grafting of methacrylic acid to the cellulose nanocrystals.

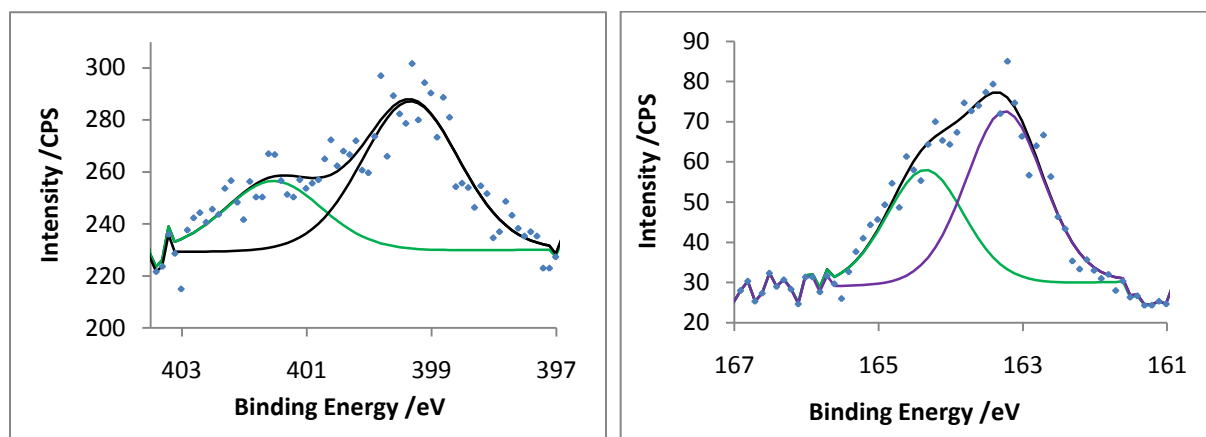


Figure S11: High resolution spectra of the N 1s (left) and S 2p (right) peaks: Amine Cellulose Nanocrystals.

| Orbital | Environment | Binding Energy /eV | FWHM | Lineshape |
|---------|-------------------------------|--------------------|------|-----------|
| N 1s | -NH ₂ | 399.3 | 1.84 | GL(30) |
| | -NH ₃ ⁺ | 401.5 | 1.84 | GL(30) |
| S 2p | 2p 3/2 | 163.3 | 1.26 | GL(30) |
| | 2p 1/2 | 164.4 | 1.26 | GL(30) |

In the XPS spectra of amine cellulose nanocrystals see small signals from sulphur and nitrogen can be observed showing the success of the thiol-ene click reaction. As the signals are very small we employed elemental analysis to determine the degree of substitution.

| Atom | Theoretical mass % | Actual mass % | DS |
|----------|--------------------|---------------|-------|
| Nitrogen | 2 | 0.25 | 0.124 |

From the elemental analysis it is clear that the small size of the signals in XPS is due to a fairly low degree of grafting of the amine groups. From these results and the grafting density of the dyes calculated below, the dyes will not be detectable in XPS. XPS characterization after grafting with dye did not show significant change in signals (apart from the apparition of a small fluorine signal for the grafting of Oregon Green 488 carboxylic acid, See Table 1) and thus, this data is not shown.

Determination of grafting density

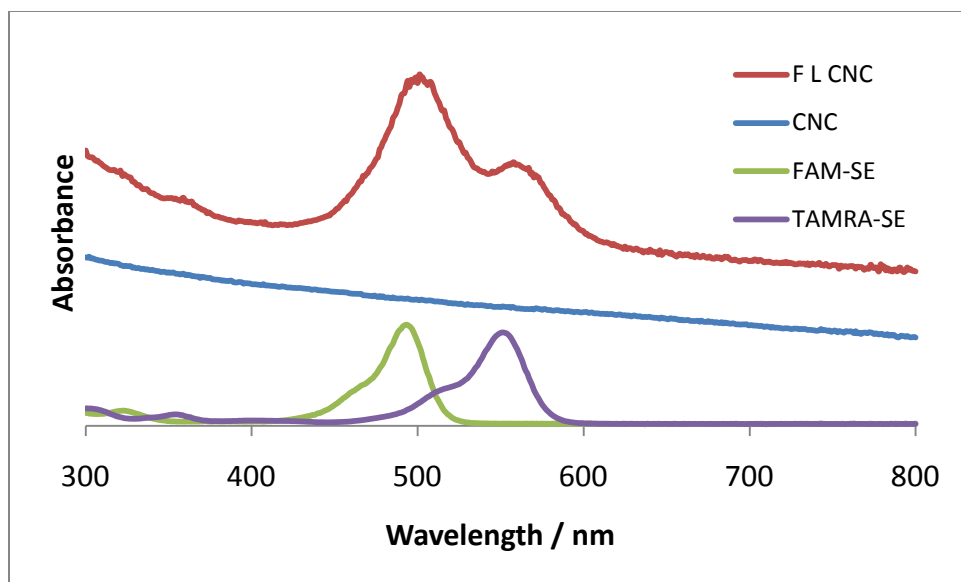


Figure S12: UV-Vis spectra of unmodified (0.1 wt %) and modified cellulose nanocrystals (0.1 wt %) and naked dye (5.0 μ M) in 50mM sodium borate buffer pH = 9.0.

The grafting density of OG-SE, FAM-SE and TAMRA-SE was determined by UV-Vis spectroscopy. As can be seen in Figure S12 the modified nanocrystals show a clear absorbance peak at 490 nm and 555 nm corresponding to OG-SE/FAM-SE and TAMRA-SE respectively, whereas the unmodified cellulose nanocrystals show no absorption peaks at these wavelengths. The grafting density was determined by relating the intensity of the peaks to a calibration curve constructed from known concentrations of the free dye in 50 mM sodium borate buffer pH = 9.0.

¹ Y. Cao and H. Tan, *Enzyme Microb. Tech.*, 2005, **36**, 314